

## A two-step synthesis of NiZn–W hexaferrites

Darja Lisjak<sup>a,\*</sup>, Andrej Žnidaršič<sup>b,1</sup>, Anna Sztanislav<sup>c</sup>, Miha Drogenik<sup>a</sup>

<sup>a</sup> Jožef Stefan Institute, Jamova 39, 1000 Ljubljana, Slovenia

<sup>b</sup> Iskra Feriti d.o.o., Stegne 29, 1000 Ljubljana, Slovenia

<sup>c</sup> TKI Ferrit, Ungvar u. 64-66, H-1142 Budapest, Hungary

Received 1 November 2007; received in revised form 28 January 2008; accepted 1 February 2008

Available online 3 April 2008

### Abstract

We have investigated the formation of single-phase NiZn–W hexaferrites using two different approaches to the synthesis: a direct synthesis from an initial reagent mixture and a two-step synthesis from intermediates. As calculated, the probability of forming single-phase powders with a direct synthesis was lower than for the two-step synthesis. Powders were synthesized with both approaches via coprecipitation followed by a calcination at 1200–1300 °C. The synthesis was monitored with X-ray powder diffraction, thermogravimetric and thermomagnetic analyses. Single-phase NiZn–W hexaferrite powders were only obtained with the two-step synthesis. The electromagnetic properties of the NiZn–W powders and ceramics were measured.

© 2008 Elsevier Ltd. All rights reserved.

**Keywords:** Powders-solid state reaction; Magnetic properties; Dielectric properties; Ferrites; Microwave applications; BaNiZnFe<sub>16</sub>O<sub>27</sub>

### 1. Introduction

Due to the ever-increasing exploitation of microwaves and the consequent saturation of the microwave bands civil applications have started to move to mm-waves. One example is collision-avoidance systems (CASs), which are basically radar modules operating at 24 and 77 GHz. These CASs have been developed to reduce the number of traffic accidents.

Some of the most important parts of radar modules are the circulators. Of the possible materials available, hexaferrites are the most suitable for applications at such frequencies. In addition, no external magnet is required due to their high magnetocrystalline anisotropy. Ba hexaferrites are complex oxides in the system BaO–Fe<sub>2</sub>O<sub>3</sub>–MeO, where Me = a bivalent transition metal.<sup>1</sup> The magnetic properties of hexaferrites can be tuned with their chemical composition and microstructure for applications in the range 1–100 GHz.<sup>2,3</sup> NiZn–W hexaferrites with the composition BaNi<sub>x</sub>Zn<sub>1-x</sub>Fe<sub>16</sub>O<sub>27</sub> are suitable for 20–30-GHz applications. The preparation of single-phase

W-hexaferrites, which requires high temperatures, is a very demanding task and it has rarely been successful.<sup>6–12</sup> In general, for all complex hexaferrites the reaction kinetics is the main problem in the synthesis and preparation of single-phase powders.<sup>8,13,14</sup> The key parameter is the homogeneity. Since all complex hexaferrites are structurally different combinations of S, R and/or T blocks, the Gibbs free energies of their formation are similar.<sup>13</sup> Consequently, the thermodynamic conditions for their formation are also similar. Therefore, a local inhomogeneity and/or non-stoichiometry in the reaction mixtures with the stoichiometry of a particular hexaferrite (e.g., W-hexaferrite = (RSS)<sub>2</sub>) can result in the formation of another hexaferrite with a slightly different combination of structural blocks (e.g., X-hexaferrite = (RS)<sub>2</sub>S).<sup>13,14</sup>

Several studies have also highlighted the problem of secondary phases, which are in fact intermediates of the complex hexaferrite.<sup>7,6,10,12</sup> Complex hexaferrites are not formed directly from oxides but via intermediates (which are structurally simpler ferrite phases) in a so-called topotactic reaction.<sup>15</sup> If the homogeneity of the reaction mixture is not perfect, the intermediate mixture is composed of regions with an excess/deficiency of one of the intermediates. Since the intermediate phases are thermodynamically stable at the reaction temperature they do not react quantitatively in a short enough time due to too slow kinetics. Consequently, we obtain multiphase powders.

\* Corresponding author. Tel.: +386 1 4773 872; fax: +386 1 4773 875.

E-mail address: [darja.lisjak@ijs.si](mailto:darja.lisjak@ijs.si) (D. Lisjak).

<sup>1</sup> Present address: Kolektor Magma d.o.o., Stegne 29, SI-1521 Ljubljana, Slovenia.

In this study we overcame this problem by employing a two-step synthesis. In the first step the very fine intermediates, M-hexaferrite and spinel, were synthesized, and from the intermediates W-hexaferrite was synthesized in the second step. In order to ensure the homogeneity, fine precursor and intermediate powders, spinel and M-hexaferrite, were prepared via the coprecipitation method. Nanosized spinel powders can be obtained after coprecipitation at room temperature<sup>16</sup> and sub-micron M-hexaferrite powders can be obtained after calcination of the coprecipitates at 700 °C.<sup>17</sup> The idea was that the probability of forming single-phase W-hexaferrite directly from the reagents was lower than for its formation from intermediates. This is shown experimentally and mathematically in the following.

## 2. Experimental procedure

W-hexaferrite with the composition  $\text{BaNiZnFe}_{16}\text{O}_{27}$  (NiZn–W) in batches of 5 g was synthesized using direct synthesis (W-1) and the two-step synthesis (W-2) via coprecipitation followed by a solid-state reaction at 1200–1300 °C. The simultaneous coprecipitation of the Ba, Fe, Zn and Ni ions was possible only with tetramethylammonium hydroxide (TMAH) at pH ~ 13. The initial solutions and filtrates were analyzed with inductively coupled plasma atomic emission spectroscopy (ICP-AES), performed with a spectrometer (ICP-AES Atomscan 25, Thermo Jarrell Ash). The content of the dissolved Zn ions in the filtrates was a maximum of 1 at.% with the respect to the stoichiometric composition. Since even lower concentrations of other ions were determined in filtrates the deviation from stoichiometric composition of coprecipitates can be neglected.

Direct synthesis (W-1): stoichiometric amounts of Ba(II) nitrate (99.95%, Alfa Aesar), Fe(III) nitrate (AR, Alfa), Ni(II) sulphate (Kemična tovarna Podnart) and Zn(II) nitrate (flakes, Alfa) were dissolved in 210 ml of water. Despite the possible coprecipitation of  $\text{BaSO}_4$  the solution remained clear and no visible precipitates were observed. The solution was added slowly to the 200 ml-water solution of TMAH with pH ≥ 13. The final pH was corrected to pH 13 with an additional amount of TMAH solution. The coprecipitates were filtered, washed with water and absolute ethanol, dried at 80 °C and calcined at 1200–1300 °C for 3 h.

Two-step synthesis (W-2): the intermediates spinel ( $\text{Ni}_{0.5}\text{Zn}_{0.5}\text{Fe}_2\text{O}_4$ ) and M-hexaferrite ( $\text{M} = \text{BaFe}_{12}\text{O}_{19}$ ) were prepared via coprecipitation in a similar way as described for W-1. The spinel crystallized at room temperature, while M was obtained after calcination at 700 °C for 2 h. A homogenized mixture of spinel and M-hexaferrite in a stoichiometric ratio was calcined at 1200–1300 °C for 3 h.

The synthesis was monitored with X-ray powder diffraction using a diffractometer with Cu  $K\alpha$  radiation (D4 Endeavor, Bruker AXS), with thermogravimetric and differential thermal analyses (TGA and DTA) using simultaneous TG/DTA/DSC apparatus (STA 449 C/6/G Jupiter<sup>®</sup>, Netzsch) and with thermomagnetic measurements using a vibrating-sample magnetometer (VSM, Lakeshore 7312). The Curie temperature ( $T_c$ ) was deter-

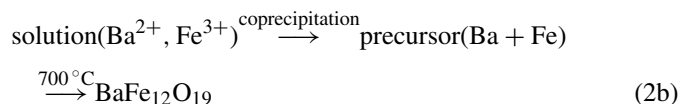
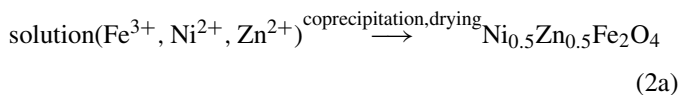
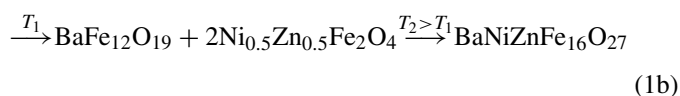
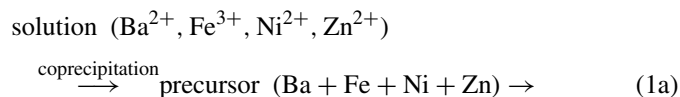
mined as the minimum of the derivative of the magnetization versus temperature. The detection limit of the ferrite phases was ≤ 0.2 wt.%.

The magnetization vs. magnetic field was also measured up to 1 T with a VSM. The dependence of the permeability on frequency was obtained from the scattering parameters<sup>18</sup> measured at 0.04–10 GHz with a vector network analyzer (Anritsu 37369C) in a coaxial line APC-7. The permittivity was measured at 9.3 GHz within a waveguide arrangement (HP 8722D Network Analyzer). While investigating the resonance frequency, the permittivity was calculated using a perturbation method.<sup>19</sup> The ceramics for the electromagnetic measurements were prepared with 2 h of preheating at 400 °C, with a heating rate of 0.5 °C/min, followed by the reaction sintering at 1300 °C for 3 h, with a heating rate of 10 °C/min. A total of 0.5 wt.% of  $\text{SiO}_2$  and  $\text{Al}_2\text{O}_3$  was added to promote the sintering and to suppress the exaggerated grain growth, which is typical for hexaferrites. The preheating was necessary for the degradation of the possible remaining nitrate, sulphate and TMAH. The microstructures were observed with the scanning electron microscope (SEM JEOL 840A) connected to a Tracor Northern Analyser for energy-dispersive-spectroscopy (EDS) analysis. The density of the ceramics was calculated from the dimensions. The same density values, within an experimental error, were obtained with Archimedes's method using Hg as an immersion liquid. The densities of the ceramics were  $4.6 \pm 0.1 \text{ g/cm}^3$ , which is around 87% of the theoretical density.

## 3. Results and discussion

### 3.1. The formation of NiZn–W

The direct synthesis of NiZn–W (W-1) involves reactions described with Eqs. (1a) and (1b). The precursor, which formed after the coprecipitation showed no distinct diffraction peaks in the corresponding X-ray diffractogram (Fig. 1). This indicates that the solid-state reaction begins from a homogeneous mixture of the amorphous Ba, Fe, Ni and Zn precursors. The two-step synthesis (W-2) can be described with Eqs. (2a)–(2c). The spinel crystallized at room temperature, while the M precursor crystallized as M-hexaferrite at 700 °C, as can be seen in the corresponding X-ray diffractograms, also shown in Fig. 1.



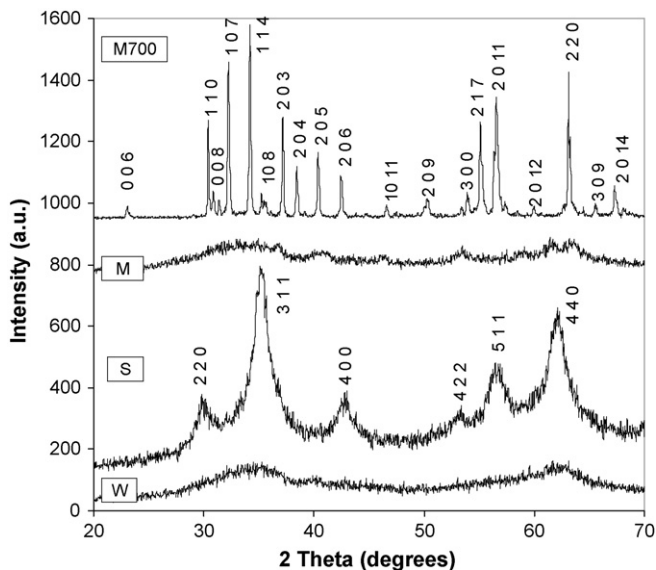


Fig. 1. X-ray diffractograms of the as-coprecipitated precursors prepared with the W-1 method (W) and with the W-2 method (S, M), and of the calcined M precursor (M700). The spinel (S) peaks are indexed according to the  $Fd3m$  (227) space group and the M-hexaferrite peaks (M700) are indexed according to the  $P6_3/mmc$  (194) space group. For the sake of clarity the indices of the minor peaks were omitted.

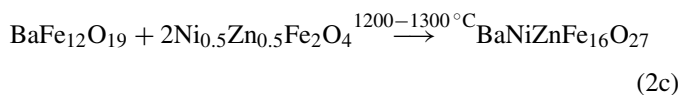


Fig. 2 shows the results of the TG/DTA of the as-coprecipitated precursor prepared with the W-1 method. A sharp exothermic peak with a maximum at 250 °C accompanied by a huge mass loss corresponds to the degradation of the leftover TMAH and/or nitrate. Such an exothermic peak and mass loss were also observed in the TG/DTA curves of the as-coprecipitated spinel and M-precursor prepared with the W-2 method. No significant mass loss can be observed above 400 °C. Due to the small sulphate (and the possible sulphate-leftover) content no significant contribution to the mass loss can be distinguished.

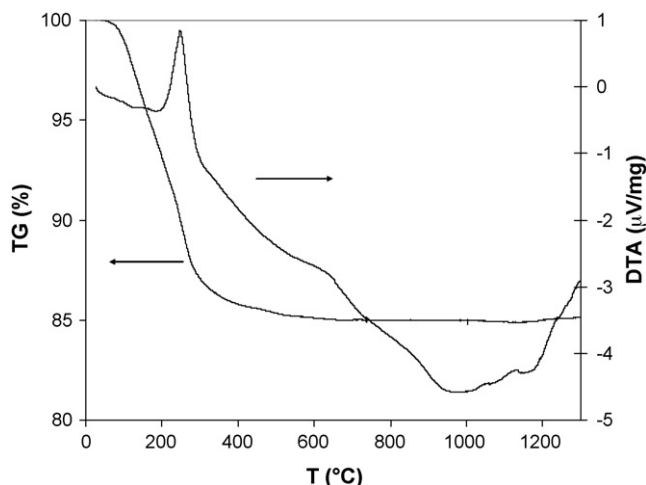


Fig. 2. TG and DTA curves of the as-coprecipitated precursor prepared with the W-1 method.

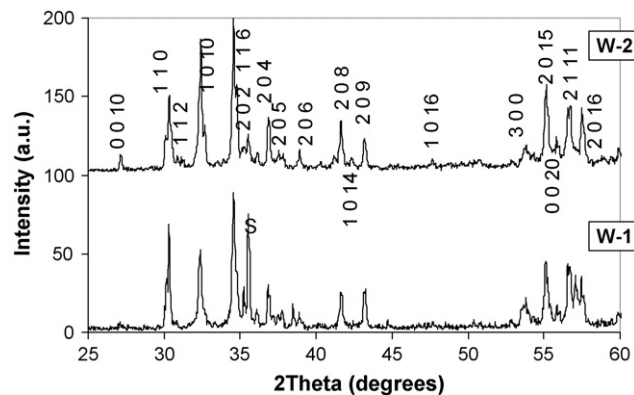


Fig. 3. X-ray diffractograms of the NiZn–W powders calcined at 1300 °C. S denotes the spinel structure, the W-hexaferrite peaks are indexed according to the  $P6_3/mc$  (194) space group.

An exothermic peak above 1200 °C can be associated with the formation of NiZn–W. The latter was confirmed with an XRD analysis. The formation of NiZn–W began at 1200 °C, but the single-phase NiZnW-hexaferrite was obtained only with the W-2 method at  $\geq 1250$  °C. In the case of the W-1 method, other structures were detected besides the W-hexaferrite. Fig. 3 shows X-ray diffractograms of the directly synthesized powder, W-1, and of the powder synthesized by the two-step synthesis, W-2. Both diffractograms correspond to the W-hexaferrite structure. An additional peak corresponding to the spinel structure can be observed in the X-ray diffractogram of the W-1 powder.

Due to the already-mentioned similarity of the different ferrite structures, some peaks of different structures overlap in the X-ray diffractogram. For example, the (3 1 1) spinel peak overlaps with the (202) W-hexaferrite peak (Fig. 3). Consequently, the detection of various ferrite structures present in minor amounts with XRD analyses is not unambiguous. Therefore, we performed thermomagnetic analyses (TMA) on all the presumably single-phase powders. The corresponding TMA curves of the NiZn–W synthesized with the W-2 method and calcined at 1250 and 1300 °C are shown in Fig. 4. For both samples only one ferrimagnetic-to-paramagnetic phase transition, i.e., Curie temperature ( $T_c$ ), can be observed. From this we can conclude that only one ferrimagnetic phase is present in the two samples. The  $T_c$  was determined at around 430 °C. Licci et al.<sup>5</sup> reported a slightly lower  $T_c$ , 423 °C, for the  $\text{BaNiZnFe}_{16}\text{O}_{27}$ . Their measurements showed an increase in the  $T_c$  with an increasing Ni content in the  $\text{BaNi}_x\text{Zn}_{1-x}\text{Fe}_{16}\text{O}_{27}$ . The  $T_c$  of around 430 °C agrees well with the composition  $\text{BaNi}_{1.1}\text{Zn}_{0.9}\text{Fe}_{16}\text{O}_{27}$ . The lower Zn content in the studied samples can be explained by the evaporation of Zn during the calcination. The latter was previously<sup>5</sup> suppressed with the use of oxygen during the calcination and sintering. The exact chemical composition of the obtained NiZn–W was not of prime importance for this study. Regardless of this, we showed that the single-phase W-hexaferrite can be obtained after 3 h of calcination at 1250 or 1300 °C only with the W-2 method. Although this result does not exclude the possibility of obtaining single-phase NiZn–W with the direct W-1 method using a longer calcination time and, maybe, a higher calcination temperature, it confirms the

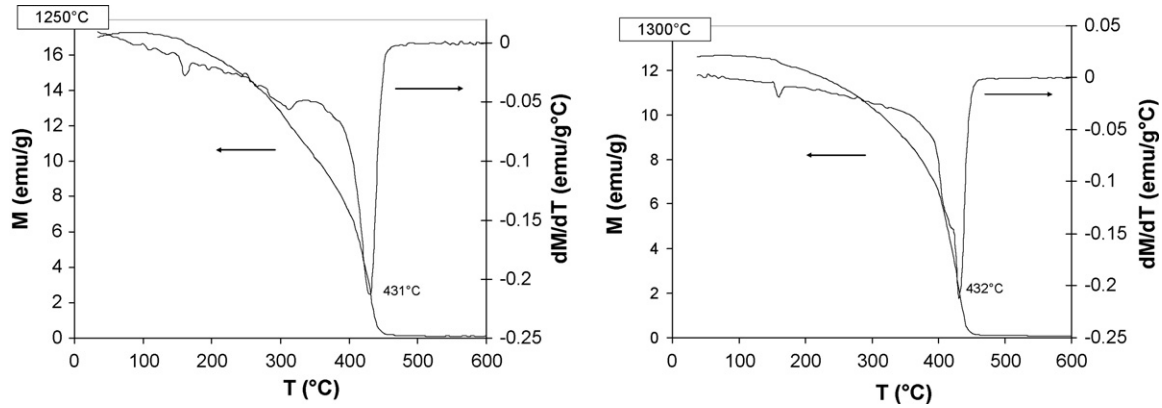


Fig. 4. TMA curves of the NiZn–W powders prepared with the W-2 method at 1250 °C and at 1300 °C.

benefits of an additional step in the synthesis with an additional homogenization of the intermediates applied in the W-2 method. This is also in agreement with our principal idea and, as shown below, with the calculated probabilities for each of the powders.

### 3.2. Probability of the formation of single-phase ZnNi-W: calculation

The probability calculations were applied, as an addition to the experimental evidence (Section 3.1). We assumed that the probability for the formation of any of the hexaferrite structures is similar due to the comparable Gibbs free energies for the formation of various hexaferrite structures (see Section 1). The type of structure that finally forms depends solely on the homogeneity: the amount and the distribution of the cations involved in the reaction. Consequently, the probability of forming single-phase NiZn–W directly from the reagents,  $P_{W-1}$ , and the probability of forming single-phase NiZn–W from intermediates,  $P_{W-2}$ , were calculated with Eqs. (3) and (4), respectively.<sup>20</sup>

$$P_{W-1} = P_{R4} P_{hf5} \quad (3)$$

$$P_{W-2} = \sum_{m=1}^4 (C_4^m)^{-1} \quad (4)$$

Here,  $P_{R4} = \sum_{m=1}^4 (C_4^m)^{-1}$  denotes the probability of the formation of a compound from all four reagents, while  $C_4^m = 4!/m!(4-m)!$  are all the possible combinations of four reagents for a compound composed from  $m$  ( $m=1-4$ ) reagents. In the same way,  $P_{hf5} = \sum_{m=1}^5 (C_5^m)^{-1}$  denotes the probability of forming only W-hexaferrite from among five possible phases (Y-, W-, X-, Z- and U-hexaferrite) composed from all four cations that could form as a single- or multi-phase powder. The probability of forming single-phase NiZn–W from the intermediates ( $P_{W-2}$ ), according to Eq. (1b), is the probability of forming a single-phase W-hexaferrite without any of the three possible secondary phases: spinel ferrite, and M- and X-hexaferrite.

As expected,  $P_{W-2}$  was higher than  $P_{W-1}$ ; 0.67 and 0.40, respectively.

### 3.3. Electromagnetic properties of the NiZn–W ceramics

Fig. 5 shows magnetic hysteresis loops of the single-phase NiZn–W samples. The magnetization values measured at 10 kOe were 66 and 62 emu/g for the samples calcined for 3 h at 1250 and 1300 °C, respectively. These values are lower than the bulk values of the saturation magnetization (around 75 emu/g)<sup>4,5</sup>. The reason for this is that the maximum magnetic field of our VSM (10 kOe) was below the value of the NiZn–W anisotropy field (11–13 kOe). It is clear from Fig. 5 that the magnetization did not saturate, but was continuously increasing up to 10 kOe. The coercivity was higher for the sample calcined at 1250 °C (530 Oe) than for the sample calcined 1300 °C (250 Oe). This is to be expected, since the hexaferrite particles usually start to grow extensively at 1300 °C. The coercivity is lower in the larger particles due to the formation of magnetic domains.

Fig. 6 shows the permeability of the NiZn–W ceramics measured at 0.04–10 GHz. A rapid decrease in the real permeability from 2.2 at 0.04 GHz to 2.0 at 1.2 GHz followed by a moderate decrease at higher frequencies can be observed. These low permeability values are to be expected for a material with a

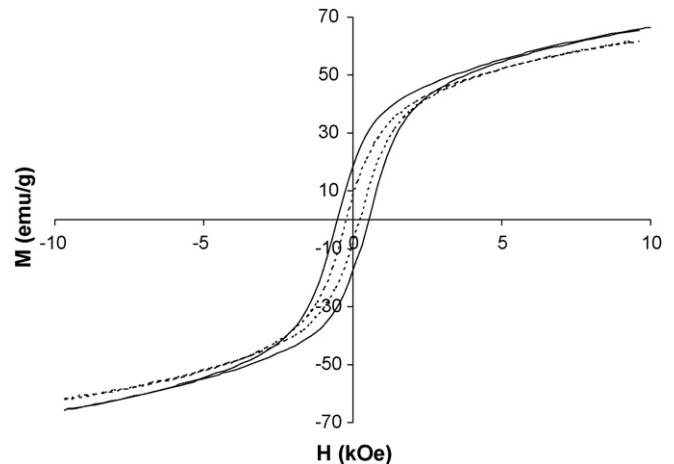


Fig. 5. Magnetization vs. magnetic field of the NiZn–W powders prepared by the W-2 method at 1250 °C (full line) and at 1300 °C (dotted line).

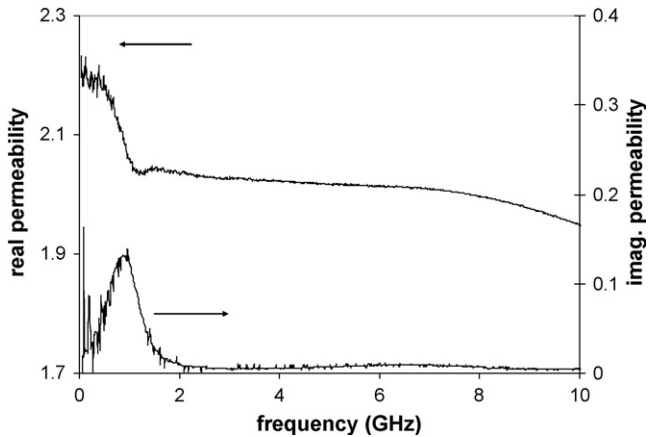


Fig. 6. Permeability vs. frequency dependence of the NiZn–W ceramics.

high magnetocrystalline anisotropy, since the permeability is inversely proportional to the anisotropy field. The imaginary part of the permeability shows a maximum at around 1 GHz. This can be attributed to domain-wall relaxation. The grain size of the ceramic (Fig. 7) was large enough for the formation of magnetic domains. As already mentioned, the ferromagnetic resonance

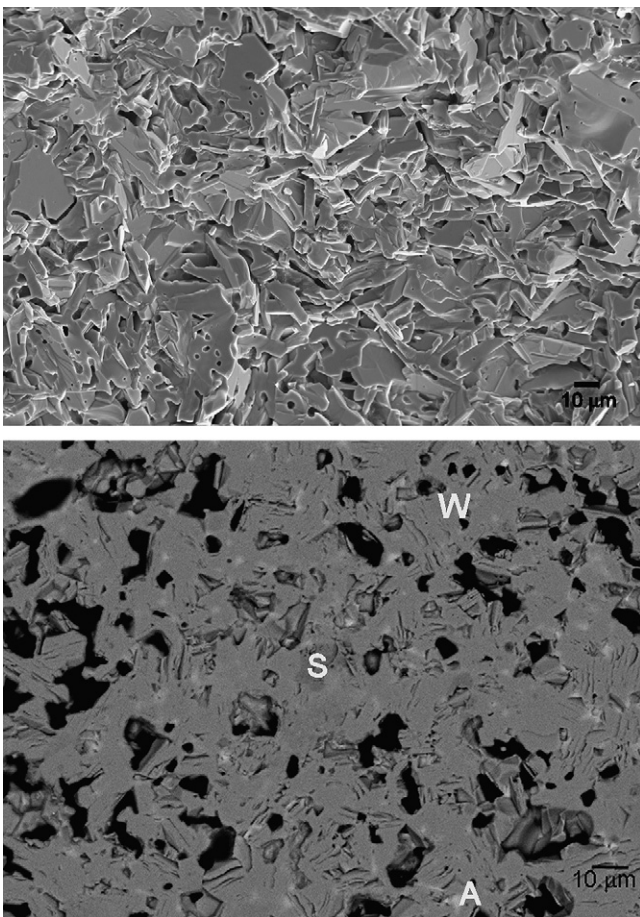


Fig. 7. Electron micrographs of the NiZn–W ceramics: secondary-electron image of the fractured surfaces (top) and backscattered-electron image of the polished surface (bottom). W denotes the W-hexaferrite phase, S denotes the spinel phase and A denotes the Si,Al-rich phase.

occurs above 30 GHz and has no influence on the permeability in the measured frequency range.

The real permittivity of the NiZn–W ceramics measured at 9.3 GHz was 14, which is a typical value for ferrites. However, the  $\text{tg } \delta$  was 0.0115, which is too high for applications in non-reciprocal devices, like circulators. The high dielectric losses can be explained by the relatively high porosity (around 13%) and by the presence of secondary phases. Besides the main W-hexaferrite phase, the spinel phase—NiZn ferrite (the dark phase marked with S) and the Si,Al-rich phase (the white phase marked with A) were also observed in the backscattered-electron image (Fig. 7). The Si,Al-rich phase originated from the used sintering additives,  $\text{SiO}_2$  and  $\text{Al}_2\text{O}_3$ . It has to be noted that Si and Al were detected only in the Si,Al-rich phase. The spinel was not detected in the powder samples using XRD and TMA. Its formation was obviously only promoted during the sintering, most likely due to the reaction between the NiZn–W and the sintering additives. The sintering will have to be optimized in future in order to decrease the dielectric losses.

#### 4. Conclusions

A two-step synthesis approach for single-phase NiZn–W hexaferrite powder was proposed. The key to the formation of single-phase powders is the homogeneity. This was increased by adding an additional step to the synthesis. The probability of the direct formation of single-phase NiZn–W hexaferrite from the reagents was 0.40, which was lower than the probability for the formation of multiphase powders. In contrast, the probability of the formation of single-phase NiZn–W hexaferrite from the intermediates was 0.67, i.e., higher than the probability for the formation of multi-phase powders. This was also observed experimentally with the synthesis based on the coprecipitation method. Single-phase NiZn–W powders were obtained only from the pre-synthesized intermediates and not directly from the precursors. The same two-step approach is also suggested for other complex hexaferrites (i.e., X, Z and U) that form via intermediates. The only condition is the need to use very fine intermediate powders. The NiZn–W powders and ceramics showed the expected electromagnetic behaviour.

#### Acknowledgements

This work was accomplished in the frame of the Eureka project E!3451 FDMA (Ferrite materials and devices for mm-wave applications) supported by the Ministry of Higher Education, Science and Technology of the Republic of Slovenia and by the Agency for Research Fund Management and Research Exploitation in Hungary. The authors would like express their gratitude to Mr Sašo Gyergyek (BSc) for the VSM measurements.

#### References

- Smit, J. and Wijn, H. P. J., Ferrites. Philips' Technical Library, Eindhoven, 1959, pp. 71–73, 177–211.

2. Pardavi-Horvath, M., Microwave applications of soft ferrites. *J. Magn. Magn. Mater.*, 2000, **215–216**, 171–183.
3. Rodrigue, P., Magnetic materials for millimeter wave applications. *IEEE Trans. Microw. Theory Tech. MTT-11*, 1963, 351–356.
4. Besagni, T., Deiru, A., Licci, F., Pareti, I. and Rinaldi, S., Nickel and copper substitution in Zn<sub>2</sub>-W. *IEEE Trans. Magn. MAG-17*, 1981, **6**, 2636–2638.
5. Licci, F., Pareti, L. and Rinaldi, S., Zn<sub>2</sub>W: improvements of magnetic properties by copper substitution. *J. Appl. Phys.*, 1981, **52**(3), 2526–2528.
6. Lotgering, F. K., Vromans, P. H. G. M. and Huyberts, M. A. H., Permanent-magnet material obtained by sintering the hexagonal ferrite W = BaFe<sub>18</sub>O<sub>27</sub>. *J. Appl. Phys.*, 1980, **51**(11), 5913–5918.
7. Leccabue, F., Panizzieri, R., Saliati, G., Albanese, G. and Sanchez Llamzares, J. L., Magnetic and morphological study of BaZn<sub>2</sub>Fe<sub>16</sub>O<sub>27</sub> hexagonal ferrite prepared by chemical coprecipitation method. *J. Appl. Phys.*, 1986, **59**(6), 2114–2118.
8. Sudakar, C., Subbana, G. N. and Kutty, T. R. N., Wet chemical synthesis of multicomponent hexaferrites by gel-to-crystallite conversion and their magnetic properties. *J. Magn. Magn. Mater.*, 2003, **263**, 253–268.
9. Pullar, R. C., Taylor, M. D. and Bhattacharya, A. K., Aligned hexagonal ferrite fibres of Co<sub>2</sub>W, BaCo<sub>2</sub>Fe<sub>16</sub>O<sub>27</sub> produced from an aqueous sol–gel process. *J. Mater. Sci.*, 1997, **32**, 873–877.
10. Sürig, C. and Hempel, K. A., Magnetic anisotropy of chemically coprecipitated Zn<sub>2</sub>W ferrite. *IEEE Trans. Magn.*, 1994, **30**(2), 997–999.
11. Zhang, H., Liu, Z., Yao, X., Zhang, L. and Wu, M., The synthesis and characterization and microwave properties of ZnCo-substituted W-type barium hexaferrite, from sol–gel precursor. *J. Sol–Gel Sci. Technol.*, 2003, **27**, 277–285.
12. Müller, R., Preparation of W-type hexaferrite particles by the glass crystallization method. *J. Magn. Magn. Mater.*, 1991, **101**, 230–232.
13. Pollert, E., Crystal chemistry of magnetic oxides part 2: hexagonal ferrites. *Prog. Cryst. Growth Charact.*, 1985, **11**, 155–205.
14. Den Broeder, F. J. A., Lattice imaging of extended defects and related phases in polycrystalline Sr(Ba)Fe<sub>18</sub>O<sub>27</sub> (Ferrous W). *J. Solid State Chem.*, 1981, **37**, 362–369.
15. Lotgering, F. K., Topotactical reactions with ferrimagnetic oxides having hexagonal crystal structures-II. *J. Inorg. Nucl. Chem.*, 1960, **16**, 100–108.
16. Čampelj, S., Makovec, D., Bele, M., Drogenik, M. and Jamnik, J., Synthesis of magnetic nanoparticles functionalized with thin layer of silica. *Mater. Technol.*, 2007, **41**(2), 103–107.
17. Lisjak, D. and Drogenik, M., The mechanism of the low-temperature formation of barium hexaferrite. *J. Eur. Ceram. Soc.*, 2007, **27**, 4515–4520.
18. Baker-Jarvis, J., Janezic, M. D., Grosvenor Jr., J. H., and Geyer, R. G., Transmission/reflection and short-circuit line methods for measuring permittivity and permeability. NIST Technical Note 1355-R. U.S. Government Printing Office, Washington, 1993.
19. Almassy, G., *Mikrohullámú kézikönyv (Microwave Reference Book)*. Műszaki Könyvkiadó, Budapest, 1973, pp. 275–285.
20. Bronštejn, J. N. and Semendjajev, K. A., *Matematični priročnik (Handbook of Mathematics)*. Tehniška založba Slovenije, Ljubljana, 1984, pp. 185–186.